Lipid accumulation and oxidative stress in the crop tissues of male and female pigeons during incubation and chick-rearing periods

P. Xie,[*,†] J. G. Zhu [ORCID],[‡] L. X. Wang [ORCID],[‡] Y. Liu [ORCID],[*,†] E. J. Diao,[*,†] D. Q. Gong [ORCID],[‡] and T. W. Liu[*,†,1]

[*]*Jiangsu Collaborative Innovation Center of Regional Modern Agriculture & Environmental Protection, Huaiyin Normal University, Huaian 223300, China;* [†]*Jiangsu Key Laboratory for Eco-Agricultural Biotechnology around Hongze Lake, Huaiyin Normal University, Huaian 223300, China;* and [‡]*College of Animal Science and Technology, Yangzhou University, Yangzhou 225009, China*

ABSTRACT The current study aimed to evaluate the changes in lipid accumulation and oxidative status in pigeon crops during different breeding stages. Forty-two pairs of adult pigeons were randomly assigned to 7 groups. Lipid droplet accumulation in pigeon crops was visualized by using oil red O staining from d 17 of incubation (**I17**) to d 7 of chick rearing (**R7**). Transmission electron microscopy analysis showed swollen mitochondria with disintegration of cristae and typical characteristics of endoplasmic reticulum stress in crop tissues at R1 compared with those at I4. During the peak of pigeon milk formation, the concentrations of reactive oxygen species, and oxidative damage markers (advanced oxidation protein products, 8-hydroxy-2 deoxyguanosine, and malondialdehyde) and the enzyme activities of total superoxide dismutase and glutathione peroxidase were all elevated significantly ($P < 0.05$). The protein concentration of B-cell lymphoma-2 associated X in crop tissues was significantly higher at R1, while the level of B-cell lymphoma-2 protein in males was the highest at I4 ($P <$ 0.05). The ratio of B-cell lymphoma-2 associated X protein (**Bax**)/B-cell lymphoma-2 (**Bcl-2**) in both male and female crops peaked at R1 ($P < 0.05$). Gene expression of the key enzymes involved in mitochondrial and peroxisomal fatty acid β-oxidation was investigated in crops. In males, the gene expression of carnitine palmitoyltransferase 1a peaked at R15, and that of carnitine palmitoyltransferase 2 increased significantly from R1 to R15 ($P < 0.05$). The mRNA abundance of long chain 3-hydroxyacyl-CoA dehydrogenase increased to the maximum value at R1 and I17 in males and females, respectively. From I17 to R7, the mRNA levels of acyl-CoA oxidase 1 and acyl-CoA oxidase 2 were decreased in pigeon crops ($P < 0.05$). Conclusively, lipid droplet accumulation was found in male and female pigeon crops from the end of incubation to the early stage of chick rearing. Although antioxidant defence and mitochondrial fatty acid β-oxidation were both mobilized, oxidative stress in crop tissues still occurred during the peak of milk formation.

Key words: pigeon, crop milk, lipid, oxidative stress, mitochondria

INTRODUCTION

The formation of pigeon milk is a fascinating biological process for this special altricial bird species. Dramatic morphological and physiological changes occur in pigeon crop tissues during milk formation. In previous studies of prolactin hormone action in vivo and in vitro, numerous lipids and proteins were found to be accumulated in crop cells accompanied by rapid and massive proliferation of the epithelial layer (Carr and James, 1931; Gillespie et al., 2011; Hu et al., 2016;

Wan et al., 2019). The gene expression levels of various transporters and key synthetases of amino acids and fatty acids were commonly upregulated from the terminal phase of incubation to the early phase of chick rearing (Xie et al., 2017, 2020). Cell keratinization and mitochondria-dependent apoptosis seem to be indispensable factors that induce the degeneration of crop cells, and these nutritive epithelial cells are finally sloughed off into the cavity to form 'milk' (Gillespie et al., 2013; Xie et al., 2021).

With only 28 days of onset to market, the maturation rate of pigeon squabs is much faster than that of other poultries (Sales and Jassens, 2002). The impressive growth performance of pigeon squabs is likely attributable to their genetics and nutritive crop milk. Crop milk is rich in protein (60% of dry matter) and fat (30% of dry matter) and extremely deficient in carbohydrates

(0.9%−1.5% of dry matter) (Dumont, 1965; Shetty et al., 1994). Numerous lipid droplets were observed in the crop epithelial layer in the chick-rearing period (Gillespie et al., 2011). Lipids are considered to be a major energy source for squabs. Twenty-one different long-chain fatty acids (**LCFAs**) were identified in crop milk by gas-liquid chromatographic analyses (Desmeth, 1980). Our previous study showed that fatty acids used in lipid biosynthesis of crop milk probably originated from both exogenous supply and de novo synthesis (Xie et al., 2017). However, excessive fat deposition in animal organs in a high-fat diet model often leads to lipid metabolism disorders and inflammatory responses (Zhang et al., 2008; Jin et al., 2019; Wang et al., 2022). For example, too much fatty residue in the mammalian liver has been implicated in lipoapoptosis, fibrosis, and steatohepatitis, which are found in nonalcoholic fatty liver disease (Luedde and Schwabe, 2011). Considerable reactive oxygen species (**ROS**) induced by lipid overload will cause the oxidative damages to cellular macromolecules (DNA, lipids, proteins, etc.) (Chen et al., 2020), and it has been found to be an important reason for the maladaptive responses (Quinlan et al., 2012; Forrester et al., 2018). Apoptosis through ROS-mediated mitochondrial pathway has been reported in various types of cells (Rehman et al., 2014; Wen et al., 2020; Feng et al., 2022). Our previous study shows that cell apoptosis may play a potential role in the desquamation of crop epithelial cell (Xie et al., 2021). A cycle of production and turnover of cornified epithelium takes nearly four hours, which ensured the continuous supply of crop milk (Gillespie et al., 2013). Cornification induced cell desquamation from the epidermis is always accompanied with notable cell apoptosis in mammals (Demerjian et al., 2008; Erman et al., 2009; Eckhart et al., 2013). Therefore, the particular hypothesis put forward here was that rapid lipid accumulation can also lead to oxidative stress in the crop tissue by affecting the antioxidant system, and ROS resulting from the stress was probably vital for pigeon milk formation.

Here we presented the analysis of pigeon crop histology, the content of oxidative damage markers and the apoptosis index. The activities of antioxidant and energy metabolizing enzymes were examined during different breeding periods. Finally, the gene expression profiles of the key enzymes involved in mitochondrial and peroxisomal fatty acid β-oxidation in crop tissues were investigated by real-time PCR.

MATERIALS AND METHODS

All procedures used in this study were approved by the Animal Care Advisory Committee of Huaiyin Normal University (Ethics approval number: E-131/2022).

Table 1. Ingredients and nutrient compositions of diet (air dry basis).

	Diet
Ingredient (g/kg)	
Corn	600
Soybean meal (44.2% CP)	234
Wheat	115
Dicalcium phosphate	12
Limestone	20
Salt	2.5
Premix[1]	10
Soybean oil	5
Lysine	0.9
Methionine	0.6
Determined analysis[2]	
DM (%)	86.37
CP (%)	16.51
EE (%)	3.51
Ash (%)	6.04
GE (MJ/kg)	16.43
Calculated level[3]	
ME (MJ/kg)	12.00
CP (%)	16.67
Calcium (%)	1.13
Available P (%)	0.34
Lysine (%)	0.89
Methionine (%)	0.31

[1]Premix provided the following (per kilogram of diet): retinyl palmitate, 2.2 mg; cholecalciferol, 0.043 mg; DL-α-tocopheryl acetate, 24 mg; menadione, 1 mg; thiamine, 3 mg; riboflavin, 13 mg; pyridoxine, 2 mg; cobalamin, 2.5 mg; nicotinic acid, 15 mg; folic acid, 0.55mg; calcium pantothenate, 7.5 mg; biotin, 0.12 mg; choline chloride, 200 mg; Cu (CuSO$_4$·5H$_2$O), 10 mg; Fe (FeSO$_4$·H$_2$O), 35 mg; Mn (MnSO$_4$·H$_2$O), 55 mg; Zn (ZnSO$_4$·H$_2$O), 35 mg; I (KI), 0.2 mg; Se (NaSeO$_3$), 0.25 mg.

[2]Values were presented as the means of triplicate per sample.

[3]Values were calculated from data provided by Feed Database in China (2010).

Animals and Housing

Totally, 42 pairs (42 males and 42 females) of 60-wk-old White King pigeons with the same oviposition interval were chosen from a pigeon farm (Kunpeng Pigeon Co., Ltd., Xuzhou, China). They were randomly assigned to 7 groups (6 pairs/each) based on different breeding stages, which included day 4 (**I4**), 10 (**I10**), and 17 (**I17**) of incubation and day 1 (**R1**), 7 (**R7**), 15 (**R15**), and 25 (**R25**) of chick-rearing. Each time point in the incubation and chick rearing in the study was started from the second egg-laying. The whole study lasted 50 d, which included a 7-d acclimation period and a 43-d experimental period (18-d incubation and 25-d chick rearing). As described in our previous study (Xie et al., 2018), plastic eggs were used to maintain the broodiness of parental pigeons after the second egg was laid. Squabs hatched from the incubator were cared for by parents after 18-d incubation. The birds were fed a pellet compound diet based on corn, soybean meal, and wheat. Ingredients and nutrient composition of diet were presented in Table 1. The nutritional levels were recommended by the previous study with some modifications (Xie et al., 2017). Feed, sand, and water were supplied ad libitum throughout the 16-h daily light.

Each of the 6 pairs was sampled at the specific breeding stage. After a 12-h fast, the birds were euthanized by cervical dislocation. Crop tissues were partly prepared

for histological examination, and partly frozen in liquid nitrogen and stored at −80°C for subsequent examination. Eggs and baby squabs were transferred to the pigeon farm to be reared by other pigeons.

Oil Red O Staining

According to the protocol of the oil red O staining kit (Solarbio, China), briefly, 10% formalin fixed crop tissues were embedded in paraffin, and 6 μm sections were prepared and washed with 60% isopropanol. The slices were stained with oil red O working solution and counterstained with haematoxylin. Finally, the slices were sealed with glycerogelatin. Tissue sections were observed and imaged under an Eclipse 80i optical microscope (Nikon, Japan).

Transmission Electron Microscope Analysis

Tissues were fixed in 2.5% glutaraldehyde solution in 0.1 M sodium cacodylate buffer (pH 7.2) overnight at 4°C, and then postfixed in a solution containing 1% osmium tetroxide for 2 h. Samples were dehydrated with gradient alcohol and treated with embedding agent and acetone. Slices were obtained by an ultramicrotome (Leica Microsystems, Germany), and then stained with uranyl acetate and lead citrate solution. Finally, the sections were examined under an H-7650B transmission electron microscope (**TEM**; Hitachi, Japan).

ROS Assay

ROS production in pigeon crop tissues was examined using 2',7'-dichlorofluorescin diacetate (**DCFH-DA**; Sigma-Aldrich, St. Louis, MO) as described by Chen et al. (2019) with some modifications. Briefly, the tissues were homogenized in 1 mM PBS buffer (pH 7.4) on ice. The homogenates were centrifuged at 10,000 × g for 5 min, and the supernatant was diluted with ice-old Locke's buffer (154 mM NaCl, 5.6 mM KCl, 3.6 mM NaHCO$_3$, 2.0 mM CaCl2, 10 mM D-glucose, and 5 mM HEPES, pH 7.4) to obtain a concentration of 10 mg tissue/mL. Then, 190 μL of supernatant was incubated with 10 μL DCFH-DA (10 μM) for 30 min at 37°C in the dark. The fluorescence intensity for the conversion of DCFH to dichlorofluorescein (**DCF**) was measured at an excitation wavelength of 485 nm and an emission wavelength of 530 nm with a microplate reader. The protein contents were determined using the Coomassie Brilliant Blue method, and the concentration of ROS in crop tissues was expressed as fluorescence intensity (**FI**) per milligram of protein.

Determination of Oxidative Damage Markers

The contents of advanced oxidation protein products (**AOPP**) and 8-hydroxy-2 deoxyguanosine (**8-OHdG**) in crop tissues were quantified by the sandwich enzyme immunoassay technique as described in the protocols of commercial kits (8-OHdG ELISA kit: Nanjing Jiancheng Bioengineering Institute, Nanjing, China; AOPP ELISA kit: Cusabio Inc., College Park, MD). Absorbance at 450 nm was measured by a microplate reader (SpectraMax M5, Molecular Devices, Sunnyvale, CA). To determine the malondialdehyde (**MDA**) level, an assay kit based on the thiobarbituric acid method (Nanjing Jiancheng Bioengineering Institute) was used. The absorbance value was recorded at a wavelength of 532 nm using a spectrophotometer (UV-2000, Unico, Instruments, Shanghai, China).

Determination of Antioxidant and Energy Metabolizing Enzymes

Crop tissues were homogenized (1:9, w/v) with ice-cold 150 mmol/L NaCl by a hand held homogenizer (IKA Works, Inc, Wilmington, NC) and then centrifuged at 3,000 × g for 15 min at 4°C. The supernatant was used to analyse the activities of enzymes, including total superoxide dismutase (**T-SOD**), catalase (**CAT**), glutathione peroxidase (**GSH-Px**), and ATPase by a microplate reader. All of the above parameters were determined with diagnostic kits (Nanjing Jiancheng Bioengineering Institute) according to the manufacturer's instructions. The staining method for Coomassie Brilliant Blue G250 was employed to analyse the protein content of the samples. One unit of SOD activity was defined as the amount of enzyme required to cause 50% inhibition of nitroblue tetrazolium chloride (**NBT**) reduction in 1 minute. One unit of CAT activity corresponds to the amount of enzyme that decomposes 1 mol of H$_2$O$_2$ per minute. One unit of GSH-Px activity was defined as the amount of enzyme that consumed glutathione (**GSH**) per minute. One unit of ATPase was defined as the amount of enzyme that produced phosphorus in an hour during ATP decomposition.

Elisa for Tissue Apoptosis Index

Protein levels of B-cell lymphoma-2 associated X protein (**Bax**) and B-cell lymphoma-2 (**Bcl-2**) in crop tissues were examined by the sandwich ELISA kits (Jiangsu Meimian Industrial Co., Ltd, Nanjing, China). Absorbance at 450 nm was measured by a microplate reader (SpectraMax M5, Molecular Devices, Sunnyvale, CA).

RNA Isolation and cDNA Synthesis

Total RNA from crop tissues was extracted by the TRIzol method. Briefly, 0.1 g of powdered sample was treated with TRIzol reagent, deproteinized by chloroform, precipitated with isopropanol, and washed twice the ethanol solution. The RNA pellet was dried and resuspended in RNase-free dH$_2$O. The concentration of RNA was measured at 260/280 nm optical density ratio. M-MLV reverse transcriptase and oligo-dT-adaptor primers (TaKaRa, Dalian, China) were used to synthesize the cDNA.

Quantitative Real-Time Reverse Transcription-PCR

The mRNA abundances of carnitine palmitoyltransferase 1a (**CPT1a**), carnitine palmitoyltransferase 2 (**CPT2**), long chain 3-hydroxyacyl-CoA dehydrogenase (**LCHAD**), acyl-CoA oxidase 1 (**ACO1**), acyl-CoA oxidase 2 (**ACO2**), acyl-CoA oxidase 3 (**ACO3**), and 18S were detected by real-time quantitative PCR (**qRT−PCR**). The primer sequences designed by Primer Premier 5.0 software were presented in Table 2. The qRT-PCR was conducted using SYBR Premix Ex Taq (TaKaRa) in a C1000 TouchTM Thermal Cycler equipped with a CFX96 real-time PCR detection system (Bio-Rad, Hercules, CA). The procedure was performed as follows: 95°C for 30 s, followed by 40 cycles of 95°C for 5 s and 60°C for 34 s. Three replicates of each sample were determined, and specificity was confirmed by melting curve analysis. Relative mRNA levels of target genes were calculated using the $2^{-\Delta\Delta Ct}$ method (Livak and Schmittgen, 2001).

Statistical Analysis

All the data were presented as the mean ± SE. The data were statistically analyzed with one-way ANOVA followed by a Duncan's post-hoc test by using SPSS 17.0 (SPSS Inc., Chicago, IL). All statements of significance were based on $P < 0.05$.

RESULTS

Lipid Accumulation in Pigeon Crop Tissue

The density of lipid droplets in male and female crop tissues detected by using red oil O staining showed a similar changing pattern (Figures 1 and 2). At the beginning of incubation, few red lipid droplets were observed in the crop tissues. The droplets increased sharply in male and female tissues at I17 and R1, and decreased after R7. At the end of chick-rearing, the lipid droplets were almost degenerated.

Ultrastructure of Pigeon Crop Tissue

TEM analysis was shown in Figure 3. Intact mitochondria with clear cristae, endoplasmic reticulum, and dense ribosomes can be observed in male and female crop tissues at I4 (Figures 3A and 3C). However, in both male and female tissues at R1, lipid droplets were produced, and mitochondria was swollen with disintegration of cristae. The endoplasmic reticulum was also expanded, and ribosomes showed a substantial reduction (Figures 3B and 3D).

Concentrations of ROS, AOPP, 8-OHdG, and MDA

The ROS concentration in male crop tissue increased significantly at I17 and R1, while in females, it was higher at R1 than at other breeding stages ($P < 0.001$; Figure 4). The contents of oxidative damage products, AOPP, 8-OHdG, and MDA in pigeon crops changed significantly with similar treads of increasing first and then decreasing during the breeding cycle. Specifically, the AOPP content in male crops reached the maximum value at I17 ($P = 0.016$), but it peaked at R1 in female crops ($P < 0.001$; Figure 5A). However, the contents of 8-OHdG and MDA in the tissue increased to their greatest levels at R1 in both males and females ($P < 0.05$; Figures 5A and 5B).

Enzyme Activities of T-SOD, GSH-Px, CAT, and ATPase

The activities of antioxidative enzymes were shown in Table 3. In male pigeons, the activities of T-SOD and GSH-Px in crop tissues were the highest at I17, while they were at R1 in female pigeons. However, there were no significant changes in the CAT activity of male and female pigeons during the different breeding stages ($P > 0.05$). ATPase activity gradually increased to the maximum level at I17 in both male and female pigeon crops, and then decreased in the chick-rearing period (Figure 6).

Table 2. Primers used for quantitative real-time PCR analysis of gene expression[1].

Target gene	Nucleotide sequence (5'→3')[2]	Acession No.	Size (bp)
CPT1a	F: GGAGAATGTAATGG CAACTGAGT	XM_021296632	220
	R: TAGTCCCTTCCCAA AAGCATCA		
CPT2	F: ATTTCTTGGTTTGG TGCCTAC	XM_021295052	132
	R: ATGTTTTGCGTTTT CATCTGT		
LCHAD	F: CTGGTGGTGAACT GCGCC	XM_013371709	103
	R: TGACACTGATGACC CTCTGGAAG		
ACO1	F: TGGCATTGAGGAG TGTCGGA	XM_005503118	246
	R: CGCACAGTCACAGA TGGAGC		
ACO2	F: GCAAAGGCTCAC TGCCACTACAT	XM_021294615	262
	R: TGAAGTCAAACGCA TCCACGA		
ACO3	F: CCTCAGTTCCTT TAGCAGCGTA	XM_005498441	303
	R: AGCCACCTTGGTA GAGCACAG		
18S	F: AGCTCTTTCTCG ATTCCGTG	AF173630	256
	R: GGGTAGGCACA AGCTGAGCC		

[1]ACO1, acyl-CoA oxidase 1; ACO2, acyl-CoA oxidase 2; ACO3, acyl-CoA oxidase 3; CPT1a, Carnitine Palmitoyltransferase 1a; CPT2, Carnitine Palmitoyltransferase 2; LCHAD, long chain 3-hydroxyacyl-CoA dehydrogenase;.

[2]F = forward; R = reverse.
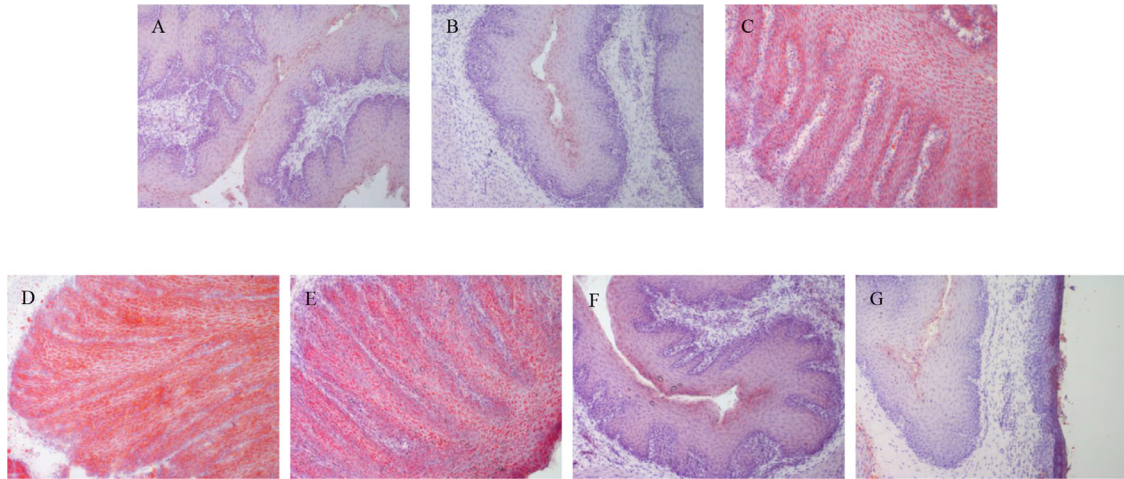
Figure 1. Lipid deposition in male crop tissues with oil red O staining in different breeding stages. The stages included incubation period: incubation d 4 (I4) (A), 10 (I10) (B) and17 (I17) (C); chick-rearing period: rearing d 1 (R1) (D), 7(R7) (E), 15 (R15) (F), and 25 (R25) (G).

Protein Concentrations of Bax and Bcl-2 and Ratio of Bax/Bcl-2

As shown in Table 4, the Bax protein concentration in crop tissues was significantly higher at R1 than at the end of chick-rearing in both male and female pigeons ($P < 0.05$). The level of Bcl-2 protein in males was the highest at I4 ($P = 0.001$), but no significant changes were observed in females ($P > 0.05$). The Bax/Bcl-2 ratio in both male and female crops reached a peak value at R1 ($P < 0.05$).

Gene Expression Levels of the Key Enzymes Involved in Mitochondrial and Peroxisomal Fatty Acid β-Oxidation

As shown in Figures 7 and 8, CPT1a gene expression gradually increased to the peak level at R15 in male pigeon crops ($P = 0.010$), while it showed no significant changes in females ($P = 0.31$; Figure 7A). CPT2 gene expression in males from R1 to R15 was 3.60 to 4.75 times higher than that at I4, but it gradually decreased to the lowest level at R25 in females (Figure 7B). The mRNA abundance of LCHAD gradually increased to the peak value at R1 and I17 in males and females ($P = 0.009$; $P = 0.005$), respectively, and then decreased to the level at the beginning of incubation (Figure 7C). From I17 to R7, the mRNA abundances of ACO1 and ACO2 were decreased. The 2 genes reached the minimum levels at I17 and R1 in male crops, respectively, but both were the lowest at R7 in female crops (Figures 8A and 8B). However, no significant changes were found in ACO3 gene expression (Figure 8C).

DISCUSSION

Marked hyperplasia in pigeon crop sacs has been detected on the 14th day of incubation (Hu et al., 2016), which is probably due to the elevation of prolactin hormone and cell factors (epidermal growth factor and
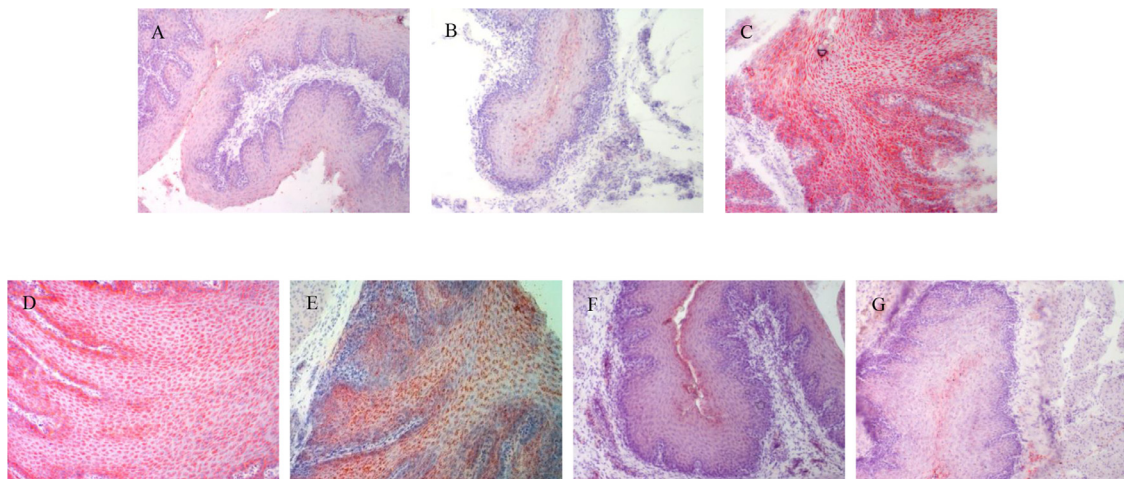
Figure 2. Lipid deposition in female crop tissues with oil red O staining in different breeding stages. The stages included incubation period: incubation d 4 (I4) (A), 10 (I10) (B), and17 (I17) (C); chick-rearing period: rearing d 1 (R1) (D), 7(R7) (E), 15 (R15) (F), and 25 (R25) (G).
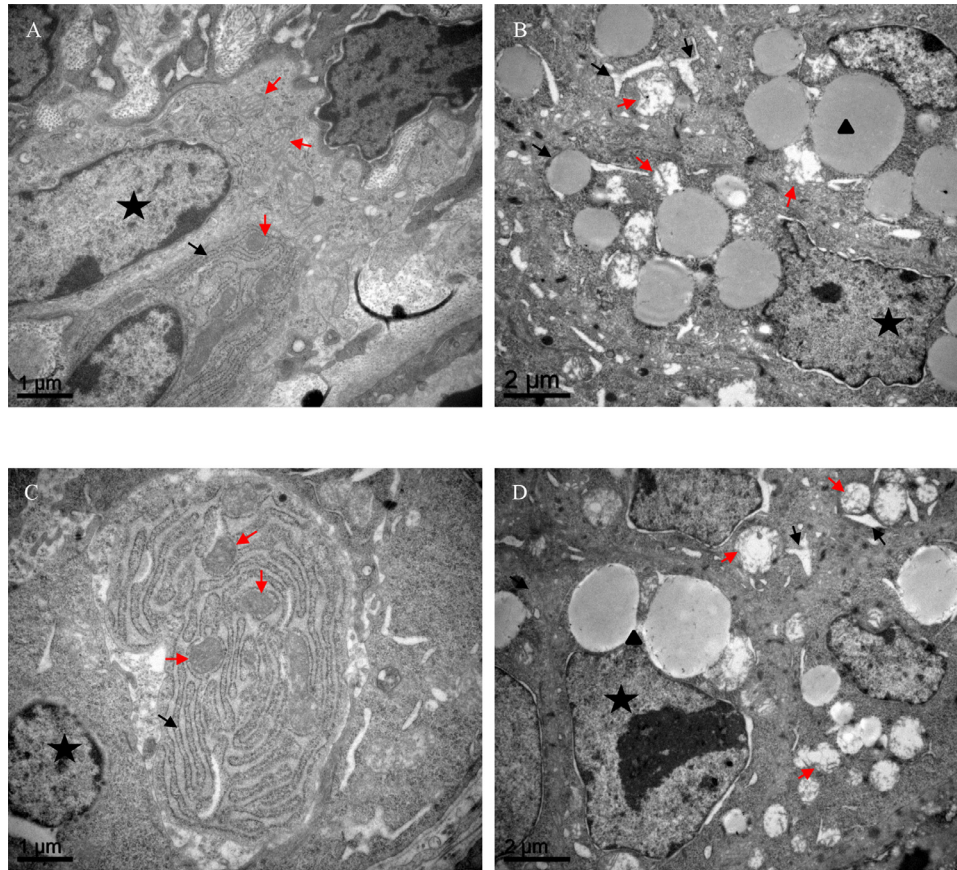
Figure 3. Ultrastructure observations of pigeon crop tissues under the transmission electron microscope (A: male crop tissue in d 4 of incubation (I4); B: male crop tissue in d 1 of chick-rearing (R1); C: female crop tissue in I4; D: female crop tissue in R1). The black pentagram indicates the nucleus. The black triangle indicates the lipid droplet. The red arrows indicate the mitochondria. The black arrows indicate the endoplasmic reticulum.

insulin-like growth factor-1) investigated in serum or crop tissue (Xie et al., 2018). It is reasonable to speculate that nutrients may also be prepared before chick rearing with the increase in crop weight and layer thickness. However, the contents of protein, fatty acids, and minerals in crop

Figure 4. Reactive oxygen species (ROS) levels in crops tissues of male and female pigeons during the different stages of incubation and chick-rearing. The stages included incubation period: incubation d 4 (I4), 10 (I10), and 17 (I17); chick-rearing period: rearing day 1 (R1), 7 (R7), 15 (R15), and 25 (R25). Values are means ± SEM (n = 6 pigeons per day for each sex). Bars with different capital letters (A, B) are significantly different in female pigeons ($P < 0.05$). Bars with different lowercases (a, b) are significantly different in male pigeons ($P < 0.05$).

milk gradually decreased during the first week of pigeon "lactation" (Shetty et al., 1990, 1992; Shetty and Hegde, 1991). In the present study, a high density of lipid droplets was observed in I17 in both male and female pigeon crops, and it decreased after R7. Genes involved in de novo lipogenesis (acetyl-CoA carboxylase and fatty acid synthase) and fatty acid transportation (fatty acid translocase, fatty acid binding protein 5, and acyl-CoA binding protein) showed significantly higher expressions from the end period of incubation to the early stage of chick rearing in our previous study (Xie et al., 2017). Therefore, the staining results can be well explained by the changing pattern of gene expression related to lipid formation. In addition, pigeon milk only can be produced until d 12 after squab hatching, and with only small quantities of milk found in crops by d 25 of lactation. This change results in a gradual transition to a whole grain diet for squabs (Vandeputte-poma, 1980). Interestingly, a considerable number of lipid droplets can still be found in male pigeons in R7 compared with females. The lipid content of crop milk in squabs reared by males was significantly higher at R4 than that from squabs reared by females (Xie et al., 2017). Our histological study again proved that sexual differences may exist in pigeon milk formation, and this was a probable physiological basis for different contributions in rearing squabs made by male and female pigeons.
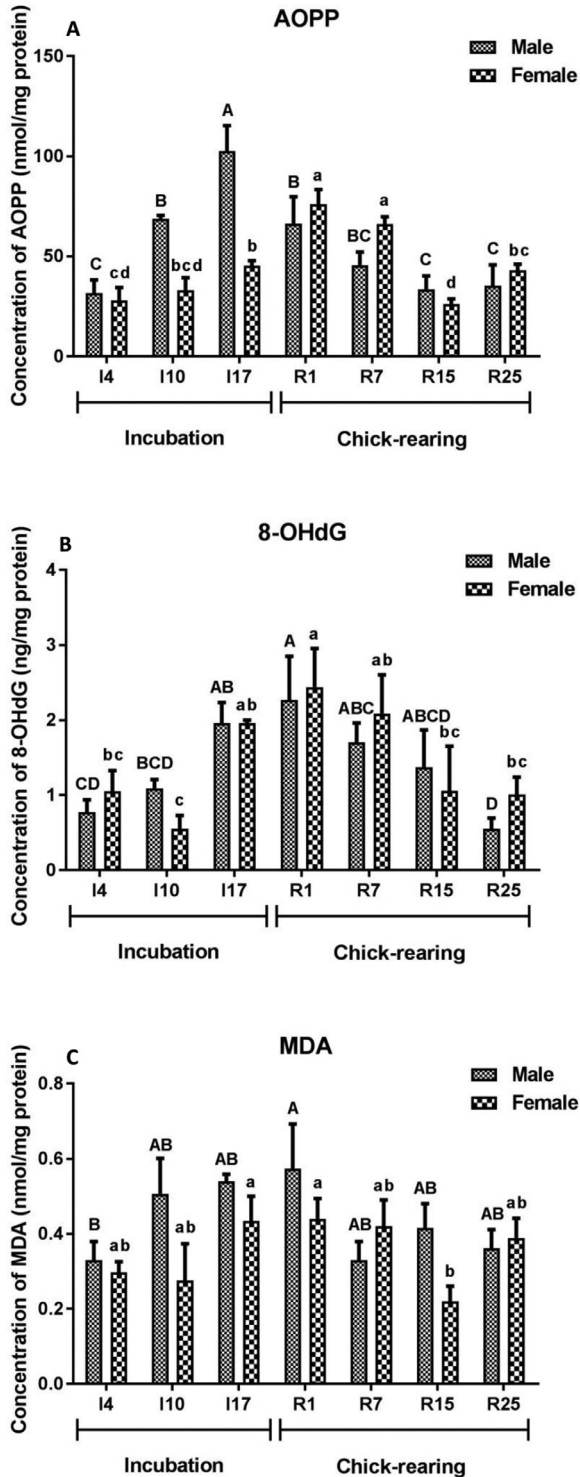
Figure 5. Concentrations of 8-hydroxy-2 deoxyguanosine (8-OHDG) (A), advanced oxidation protein products (AOPP) (B), and Malondialdehyde (MDA) (C), in crop tissues of male and female pigeons during the different stages of incubation and chick-rearing. The stages included incubation period: incubation d 4 (I4), 10 (I10), and17 (I17); chick-rearing period: rearing d 1 (R1), 7(R7), 15 (R15), and 25 (R25). Values are means ± SEM (n = 6 pigeons per day for each sex). Bars with different capital letters (A, D) are significantly different in female pigeons ($P < 0.05$). Bars with different lowercases (a, d) are significantly different in male pigeons ($P < 0.05$).

Compared with the ultramicrostructure of crop epithelial cells at I4, lipid droplets and typical characteristics of endoplasmic reticulum stress (**ERS**) with endoplasmic reticulum (**ER**) lumen expansion and

ribosome abscission, can be clearly observed at R1 by TEM analysis. The endoplasmic reticulum is an important site for protein and lipid synthesis in cells. When cells are stimulated by signals such as hormones, toxic substances, oxidative stress, nutrient deficiency or overload, unfolded or misfolded proteins accumulate excessively in organelles to induce the occurrence of ERS, and cause the unfolded protein response (**UPR**) to achieve self-protection (Rutkowski and Kaufman, 2004). To ensure the rapid growth and development of squabs, it takes only 4 h for crop epithelial cells to differentiate and slough off from the tissue (Gillespie et al., 2011). Our previous studies found that, similar to lipid formation, the expression of amino acid transporter and synthase related genes in pigeon crop tissue at the early stage of feeding was abnormally active (Xie et al., 2020). We speculated that the massive and rapid synthesis of protein caused a great stress on the metabolism of pigeon crop epithelial organelles, and ERS is likely to appear and lead to the UPR response.

Mitochondria is an important site of fatty acid β-oxidation in the majority of cell types, and contributes more than 90% of oxygen consumption in the respiratory chain (Taylor, 2008). High fat intake in animals often produces a large amount of reactive oxygen species (**ROS**) in the liver or skeletal cells through mitochondrial oxidative decomposition (Du et al., 2012). The present study showed that the ROS concentration in pigeon crop tissues notably increased during the peak of milk formation. Therefore, oxidative stress was inevitable due to the massive lipid accumulation. Macromolecules (proteins, DNA, and lipids) will be easily attacked by increasing ROS. AOPP, 8-OHdG, and MDA are typical biomarkers of oxidative stress for macromolecule damage. Advanced oxidation protein products are dityrosine-containing and cross-linking protein products generated during oxidative stress (Guo et al., 2008; Wei et al., 2009). Hydroxyl free radicals can react with DNA causing the hydroxylation of guanine at the C-8 position (Floyd et al., 1986). 8-OHdG cleaved from DNA is taken as a marker for assessing oxidative DNA damage in ROS-mediated diseases (Kasai, 1997). Lipid peroxidation affects polyunsaturated fatty acids in cell membranes, resulting in the generation of conjugated dienes and MDA (Janero, 1990). In pigeon crops, all these markers increased from the end of incubation to early chick-rearing, which suggested the ROS-induced oxidative stress. However, the time point of peak value of ROS and AOPP was different between the male and female pigeons in the present study, and the reason for the sexual difference still needed further researches.

Specific enzymes (SOD, CAT, and GSH-Px) for the detoxification of ROS protect against damage to macromolecules (Maes et al., 2011). Commonly, a decline in antioxidative defence with increased ROS generation was reported to be linked to mitochondrial dysfunction and cell apoptosis (Chen et al., 2020). Interestingly, although both the contents of ROS and oxidative damage markers increased from I17 to R1, the activities of T-SOD and GSH-Px in crop tissues were also enhanced

Table 3. Enzyme activities of total superoxide dismutase (T-SOD), catalase (CAT), and glutathione peroxidase (GSH-Px) in crop tissues of male and female pigeons during different stages of incubation and chick-rearing period.

Item[1]	Incubation (d)			Chick-rearing (d)				SEM	P value
	4	10	17	1	7	15	25		
T-SOD (U/mg protein)									
Male	32.67[ab]	36.03[ab]	47.69[a]	25.21[b]	25.60[b]	32.41[ab]	24.40[b]	2.45	0.042
Female	32.14[b]	25.11[b]	36.64[ab]	46.43[a]	25.00[b]	28.42[b]	33.38[b]	2.02	0.027
CAT (U/mg protein)									
Male	3.16	4.94	2.50	3.62	4.59	3.17	4.22	0.25	0.065
Female	3.09	4.09	3.33	2.86	2.46	2.06	2.68	0.21	0.221
GSH-Px (U/mg protein)									
Male	51.91[ab]	41.67[b]	67.25[a]	42.47[b]	47.96[ab]	52.07[ab]	39.44[b]	2.93	0.039
Female	46.06[ab]	32.44[b]	41.50[ab]	60.73[a]	39.75[ab]	47.48[ab]	53.53[ab]	3.03	0.045

[1]CAT = catalase; GSH-Px = glutathione peroxidase; T-SOD = total superoxide dismutase.
[a-b]Mean values within the same row not sharing a common superscript letter are significantly different ($P < 0.05$).

in this period. Therefore, excessive ROS production seemed to exceed the scavenging capacity of the antioxidant system, particularly during the peak of pigeon milk formation. The mitochondrial injury observed in the present study induced the inhibition of respiratory chain transmission, and promoted the production of ROS (Demeilliers et al., 2002; Zorov et al., 2006). Free radicals produced by the mitochondrial respiratory chain act on the lipid structure of the ER membrane to make it superoxidized and cause a further disorder of protein translation. The accumulation of unfolded proteins is promoted, and ERS is aggravated (Chan et al., 2016; Dilshara et al., 2017). Protein kinase R-like ER kinase (**PERK**), as an ER transmembrane protein, can trigger the downstream CCAAT/enhancer binding protein homologous protein (**CHOP**) pathway followed by the inhibition of the synthesis of intracellular glutathione, and finally amplifies the production of ROS (Yoon-Hee, 2015).

ATPase is essential for energy production in cellular functions. The synthesis and secretion of crop milk are both processes that consume energy (March et al.,

Figure 6. ATPase enzyme activities in crops tissues of male and female pigeons during the different stages of incubation and chick-rearing. The stages included incubation period: incubation d 4 (I4), 10 (I10), and17 (I17); chick-rearing period: rearing d 1 (R1), 7(R7), 15 (R15), and 25 (R25). Values are means ± SEM (n = 6 pigeons per day for each sex). Bars with different capital letters (A, C) are significantly different in female pigeons ($P < 0.05$). Bars with different lowercases (a, d) are significantly different in male pigeons ($P < 0.05$).

1978). In our study, ATPase activity in crop tissue increased to the maximum before regurgitation, but then dramatically decreased during the whole period of chick rearing. It is speculated that the elevation of ATPase activity is adapted for the development and hyperplasia of crops, and it declines as the tissue recovers to the nonlactation level.

Bcl-2-family members (Bcl-2, Bax, Bcl-w, and Bcl-x) are crucial integrators of signals for mitochondria-dependent programmed cell death (Kaufmann et al., 2004). Cell apoptosis can be inhibited by interacting and forming inactivating heterodimers with Bax/Bak (Diaz et al., 1997). In our study, the peak value of the Bax/Bcl-2 ratio at R1 as a result of higher expression of Bax together with lower Bcl-2 expression indicated that intense mitochondria-dependent cell apoptosis occurred in pigeon crops. Mitochondrial stress is specifically manifested as the improvement of membrane permeability and mitochondrial swelling, which eventually cause morphological damage and dysfunction (Singh et al., 2012). Swollen mitochondria with disintegration of cristae were observed at R1 in the present study, as reported in the skeletal muscle of animals induced by high-fat diet (Choi et al., 2018). The membrane permeability of mitochondria is regulated by Bcl-2 family members, and the activation of initiator caspases and effector caspases is triggered sequentially. Caspase-3 and caspase-9 gene expression levels peaked at d 1 of chick rearing (Xie et al., 2021). The mitochondria-dependent process possibly contributed to the desquamation to form pigeon milk.

The substrate spectra of the 2 fatty acid oxidation systems partly overlap. Mitochondria oxidize short chain (**SCFAs**, $< C_8$), the major portion of medium (**MCFAs**, C_8-C_{12}) and long chain fatty acids (**LCFAs**, C_{12}-C_{18}; Mannaerts and DeBeer, 1982). Peroxisomal β-oxidation is primarily responsible for the oxidation of very long-chain fatty acids (**VLCFAs**, $> C_{18}$) in mammals (Hardwick et al., 2009). LCFAs constitute the bulk of fatty acids in crop milk (Desmeth, 1980), and their abundances make them the important source of metabolic fuel for mitochondria. CPT1a, CPT2, and LCHAD are key enzymes for mitochondrial fatty acid β-oxidation, and they are responsible for the entry of substrates
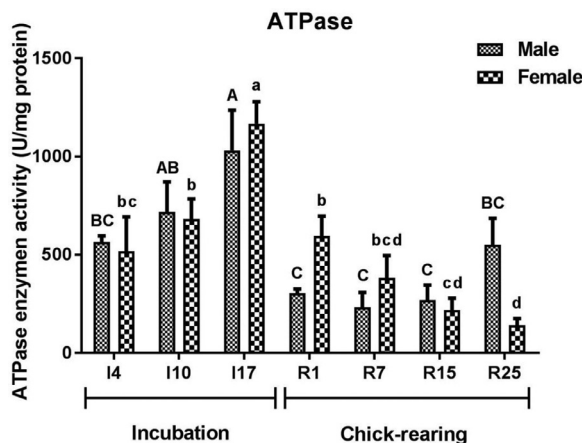
Table 4. Protein levels of B-cell lymphoma-2 associated X (Bax) and B-cell lymphoma-2 (Bcl-2) and Bax/Bcl-2 ratio in crop tissues of male and female pigeons during different stages of incubation and chick-earing period.

Item[1]	Incubation (d)			Chick-rearing (d)				SEM	P value
	4	10	17	1	7	15	25		
Bax (ng/mg protein)									
Male	33.04[ab]	23.15[bc]	28.29[abc]	35.40[a]	25.87[abc]	19.62[c]	18.53[c]	1.67	0.014
Female	21.65[c]	14.02[cd]	19.65[cd]	45.74[a]	31.27[b]	12.20[d]	15.62[cd]	2.60	<0.001
Bcl-2 (ng/mg protein)									
Male	0.77[a]	0.47[b]	0.43[b]	0.32[b]	0.38[b]	0.48[b]	0.37[b]	0.035	0.001
Female	0.42	0.43	0.54	0.62	0.43	0.78	0.55	0.039	0.091
Bax/Bcl-2 ratio									
Male	42.94[b]	50.06[b]	66.39[ab]	109.43[a]	73.23[ab]	44.27[b]	54.73[ab]	6.11	0.017
Female	52.95[ab]	33.71[bc]	38.35[bc]	74.70[a]	72.82[a]	16.82[c]	30.26[c]	5.12	<0.001

[1]Bax, B-cell lymphoma-2 associated X; Bcl-2, B-cell lymphoma-2.
[a-d]Mean values within the same row not sharing a common superscript letter are significantly different ($P < 0.05$).

into mitochondria and the final oxidation. In animal models of high-fat feeding, triglyceride (**TG**) in liver or skeletal muscle cells cannot be packaged into VLDL and transported out of the cells in time, and exceed the oxidative capacity of mitochondria, which finally results in lipid accumulation (Francone et al., 1991; Gonçalves et al., 2014). Unexpectedly, despite the oxidative damage in mitochondria, the increase in the gene expression of the 3 enzymes in male pigeons in the early stage of chick rearing indicated the active transportation and oxidation of fatty acids. Sexual differences were also found, and transportation of fatty acids in the mitochondria of female pigeons may be more stable due to CPT1a and CPT2 gene expression during the peak of milk formation. ACO catalyses the first and rate-limiting step of peroxisomal β-oxidation. Three subtypes of ACO
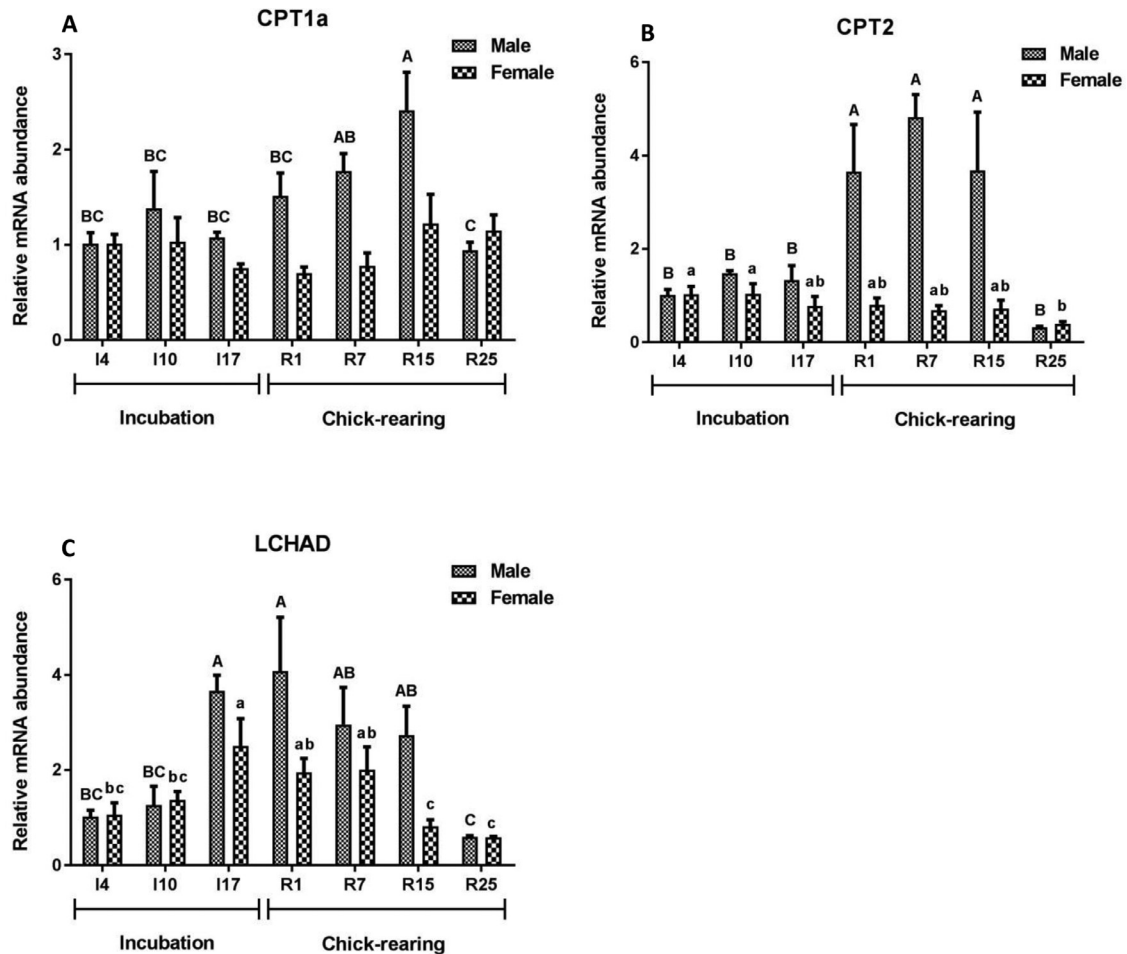
Figure 7. The mRNA expression of carnitine Palmitoyltransferase 1a (CPT1a) (A), carnitine Palmitoyltransferase 2 (CPT2) (B), and long chain 3-hydroxyacyl-CoA dehydrogenase (LCHAD) (C), in crop tissues of male and female parent pigeons during incubation and chick-rearing periods. The stages included incubation period: incubation d 4 (I4), 10 (I10), and17 (I17); chick-rearing period: rearing d 1 (R1), 7(R7), 15 (R15), and 25 (R25). Values are means ± SEM (n = 6 males and females). Bars with the different capital letters (A-C) or lowercase letters (a-c) are significantly different ($P < 0.05$).
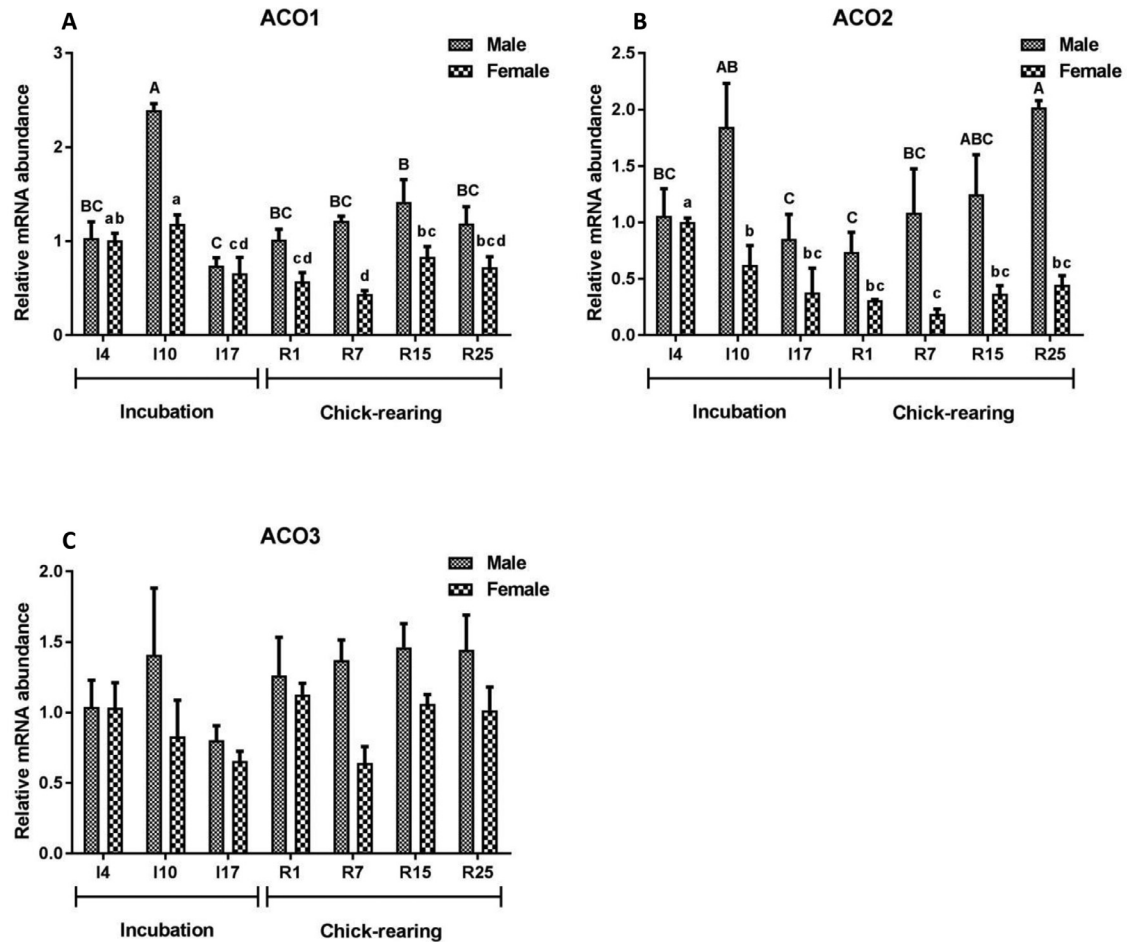
Figure 8. The mRNA expression of acyl-CoA oxidase 1 (ACO1) (A), acyl-CoA oxidase 2 (ACO2) (B), acyl-CoA oxidase 3 (ACO3) (C), in crop tissues of male and female parent pigeons during incubation and chick-rearing periods. The stages included incubation period: incubation d 4 (I4), 10 (I10) and17 (I17); chick-rearing period: rearing day 1 (R1), 7(R7), 15 (R15), and 25 (R25). Values are means ± SEM (n = 6 males and females). Bars with the different capital letters (A-C) or lowercase letters (a-d) are significantly different ($P < 0.05$).

(ACO1, ACO2, and ACO3) have been identified in rodents with different oxidized substrates and tissue distributions. The ACO2 gene is mainly expressed in the liver, while ACO1 and ACO3 can be found in various tissues (Schepers et al., 1990). In the present study, all 3 subtypes of ACO genes were detected in pigeon crops, and the expression levels of ACO1 and ACO2 were decreased during the peak of milk formation. The massive production of ROS in pigeon crops seemed to inhibit the peroxisomal β-oxidation, but not mitochondrial β-oxidation.

CONCLUSIONS

Lipid droplet accumulation was found in male and female pigeon crops from the end of incubation to the early stage of chick rearing. Mitochondrial injury and ERS were shown in crop epithelial cells at R1 under TEM analysis. Mitochondria-dependent cell apoptosis was involved in pigeon milk formation. Peroxisomal fatty acid β-oxidation was probably depressed during crop milk formation. Although antioxidant defence and mitochondrial fatty acid

β-oxidation were both mobilized, oxidative stress with higher concentrations of ROS and oxidative damage products in crop tissues still occurred during the peak of milk formation.

DISCLOSURES

No conflict of interest exits in the submission of this manuscript (Lipid accumulation and oxidative stress in the crop tissues of male and female pigeons during incubation and chick-rearing periods). We

declare that we do not have any commercial or associative interest that represents a conflict of interest in connection with the present work submitted and manuscript is approved by all authors for publication.

SUPPLEMENTARY MATERIALS

Supplementary material associated with this article can be found in the online version at doi:10.1016/j.psj.2022.102289.

REFERENCES

Carr, R. H., and C. M. James. 1931. Synthesis of adequate protein in the glands of the pigeon crop. Am. J. Physiol. 97:227–231.

Chan, C. M., D. Y. Huang, Y. P. Huang, S. H. Hsu, and W. W. Lin. 2016. Methylglyoxal induces cell death through endoplasmic reticulum stress-associated ROS production and mitochondrial dysfunction. J. Cell. Mol. Med. 20:1749–1760.

Chen, Z., R. Tian, Z. She, J. Cai, and H. Li. 2020. Role of oxidative stress in the pathogenesis of nonalcoholic fatty liver disease. Free Radic. Biol. Med. 152:116–141.

Chen, X., Y. Zhang, S. Jiang, and S. Huang. 2019. Maduramicin induces apoptosis through ROS-PP5-JNK pathway in skeletal myoblast cells and muscle tissue. Toxicology 424:152239.

Choi, J. W., J. H. Ohn, H. S. Jung, Y. J. Park, H. C. Jang, S. S. Chung, and K. S. Park. 2018. Carnitine induces autophagy and restores high-fat diet-induced mitochondrial dysfunction. Metabolism 78:43–51.

Demeilliers, C., C. Maisonneuve, A. Grodet, A. Mansouri, R. Nguyen, M. Tinel, P. Letteron, C. Degott, G. Feldmann, D. Pessayre, and B. Fromenty. 2002. Impaired adaptive resynthesis and prolonged depletion of hepatic mitochondrial DNA after repeated alcohol binges in mice. Gastroenterology 123:1278–1290.

Demerjian, M., J. P. Hachem, E. Tschachler, G. Denecker, W. Declercq, P. Vandenabeele, T. Mauro, M. Hupe, D. Crumrine, T. Roelandt, E. Houben, P. M. Elias, and K. R. Feingold. 2008. Acute modulations in permeability barrier function regulate epidermal cornification: role of caspase-14 and the protease-activated receptor type 2. Am. J. Pathol. 172:86–97.

Desmeth, M. 1980. Lipid composition of pigeon cropmilk-II. Fatty acids. Comp. Biochem. Physiol. Part B: Biochem. Mol. Biol. 66:135–138.

Diaz, J. L., T. Oltersdorf, W. Horne, M. McConnell, G. Wilson, S. Weeks, T. Garcia, and L. C. Fritz. 1997. A common binding site mediates heterodimerization and homodimerization of bcl-2 family members. J. Biol. Chem. 272:11350–11355.

Dilshara, M. G., R. G. P. T. Jayasooriya, I. M. N. Molagoda, J. W. Jeong, and Y. H. Choi. 2017. Silibinin sensitizes TRAIL-mediated apoptosis by upregulating DR5 through ROS-induced endoplasmic reticulum stress-Ca^{2+}-CaMKII-Sp1 pathway. Oncotarget 9:10324–10342.

Du, Z., Y. Yang, Y. Hu, Y. Sun, S. Zhang, W. Peng, Y. Zhong, X. Huang, and W. Kong. 2012. A long-term high-fat diet increases oxidative stress, mitochondrial damage and apoptosis in the ear of D-galactose-induced aging rats. Hear. Res. 287:15–24.

Dumont, J. N. 1965. Prolactin-induced cytologic changes in the mucosa of the pigeon crop during crop-"milk" formation. Z. Zellforsch. Mikrosk. Anat. 68:755–782.

Eckhart, L., S. Lippens, E. Tschachler, and W. Declercq. 2013. Cell death by cornification. BBA-Mol. Cell Res. 1833:3471–3480.

Erman, A., D. Zupancic, and K. Jezernik. 2009. Apoptosis and desquamation of urothelial cells in tissue remodeling during rat postnatal development. J. Histochem. Cytochem. 57:721–730.

Feng, W., J. Wang, B. Li, Y. Liu, D. Xu, K. Cheng, and J. Zhuang. 2022. Graphene oxide leads to mitochondrial-dependent apoptosis by activating ROS-p53-mPTP pathway in intestinal cells. Int. J. Biochem. Cell Biol. 146:106206.

Floyd, R. A., J. J. Watson, J. Harris, M. West, and P. K. Wong. 1986. Formation of 8-hydroxydeoxyguanosine, hydroxyl free radical adduct of DNA in granulocytes exposed to the tumor promoter, tetradeconylphorbolacetate. Biochem. Biophs. Res. Commun. 137:841–846.

Forrester, S. J., D. S. Kikuchi, M. S. Hernandes, Q. Xu, and K. K. Griendling. 2018. Reactive oxygen species in metabolic and inflammatory signaling. Circ. Res. 122:877–902.

Francone, O. L., A. D. Kalopissis, and G. Griffaton. 1991. Concomitant inhibition of VLDL triglyceride and apoprotein secretion by hepatocytes of rats adapted to a high-fat diet. Adv. Exp. Med. Biol. 285:325–328.

Gillespie, M. J., T. M. Crowley, V. R. Haring, S. L. Wilson, J. A. Harper, J. S. Payne, D. Green, P. Monaghan, J. A. Donald, K. R. Nicholas, and R. J. Moore. 2013. Transcriptome analysis of pigeon milk production - role of cornification and triglyceride synthesis genes. BMC Genomics 14:169–181.

Gillespie, M. J., V. R. Haring, K. A. McColl, P. Monaghan, J. A. Donald, K. R. Nicholas, R. J. Moore, and T. M. Crowley. 2011. Histological and global gene expression analysis of the 'lactating' pigeon crop. BMC Genomics 12:452–461.

Gonçalves, I. O., E. Passos, S. Rocha-Rodrigues, C. V. Diogo, J. R. Torrella, D. Rizo, G. Viscor, E. Santos-Alves, I. Marques-aleixo, P. J. Oliveira, A. Ascensão, and J. Magalhães. 2014. Physical exercise prevents and mitigates non-alcoholic steatohepatitis-induced liver mitochondrial structural and bioenergetics impairments. Mitochondrion 15:40–51.

Guo, Z. J., H. X. Niu, F. F. Hou, L. Zhang, N. Fu, R. Nagai, X. Lu, B. H. Chen, Y. X. Shan, J. W. Tian, R. H. Nagaraj, D. Xie, and X. Zhang. 2008. Advanced oxidation protein products activate vascular endothelial cells via a RAGE-mediated signaling pathway. Antioxid. Redox Signal. 10:1699–1712.

Hardwick, J. P., O. H. Douglas, W. Homer, M. A. Abdelmegeed, and B. J. Song. 2009. PPAR/RXR regulation of fatty acid metabolism and fatty acid ω-hydroxylase (CYP4) isozymes: implications for prevention of lipotoxicity in fatty liver disease. PPAR Res 2009:952734.

Hu, X. C., C. Q. Gao, X. H. Wang, H. C. Yan, Z. S. Chen, and X. Q. Wang. 2016. Crop milk protein is synthesised following activation of the IRS1/Akt/TOR signalling pathway in the domestic pigeon (*Columba livia*). Br. Poult. Sci. 57:855–862.

Janero, D. R. 1990. Malondialdehyde and thiobarbituric acid reactivity as diagnostic indices of lipid peroxidation and peroxidative tissue injury. Free Radic. Biol. Med. 9:515–540.

Jin, M., T. Pan, D. R. Tocher, M. B. Betancor, O. Monroig, Y. Shen, T. Zhu, P. Sun, L. Jiao, and Q. Zhou. 2019. Dietary choline supplementation attenuated high-fat diet-induced inflammation through regulation of lipid metabolism and suppression of NFkappaB activation in juvenile black seabream (*Acanthopagrus schlegelii*). J. Nutr. Sci. 8:1–11.

Kasai, H. 1997. Analysis of a form of oxidative DNA damage, 8-hydroxy-2'-deoxyguanosine, as a marker of cellular oxidative stress during carcinogenesis. Mutat. Res. Rev. Mutat. Res. 387:147–163.

Kaufmann, T., A. Schinzel, and C. Borner. 2004. Bcl-w(edding) with mitochondria. Trends Cell Biol 14:8–12.

Livak, K. J., and T. D. Schmittgen. 2001. Analysis of relative gene expression data using real-time quantitative PCR and the 2(-Delta Delta C(T)) Method. Methods 25:402–408.

Luedde, T., and R. F. Schwabe. 2011. Nf-κB in the liver—linking injury, fibrosis and hepatocellular carcinoma. Nat. Rev. Gastroenterol. Hepatol. 8:108–118.

Maes, M., P. Galecki, Y. S. Chang, and M. Berk. 2011. A review on the oxidative and nitrosative stress (O&NS) pathways in major depression and their possible contribution to the (neuro) degenerative processes in that illness. Prog. Neuro-Psychopharmacol. Biol. Psychiatry. 35:676–692.

Mannaerts, G. P., and L. DeBeer. 1982. Mitochondria1 and peroxisomal β-oxidation of fatty acids in rat liver. Ann. N. Y. Acad. Sci. 386:30–39.

March, G. L., B. A. McKeown, T. M. John, and J. C. George. 1978. Diurnal variation in circulating levels of free fatty acids and growth hormone during crop gland activity in the pigeon (*Columba livia*). Comp. Biochem. Physiol. Part B: Biochem. Mol. Biol. 59:143–145.

Quinlan, C. L., A. L. Orr, I. V. Perevoshchikova, J. R. Treberg, B. A. Ackrell, and M. D. Brand. 2012. Mitochondrial complex II can generate reactive oxygen species at high rates in both the forward and reverse reactions. J. Biol. Chem. 287:2755–27264.

Rehman, M. U., P. Jawaid, Y. Yoshihisa, P. Li, Q. L. Zhao, K. Narita, T. Katoh, T. Kondo, and T. Shimizu. 2014. Spiruchostatin A and B, novel histone deacetylase inhibitors, induce apoptosis through reactive oxygen species-mitochondria pathway in human lymphoma U937 cells. Chem.-Biol. Interact. 221:24–34.

Rutkowski, D. T., and R. J. Kaufman. 2004. A trip to the ER: coping with stress. Trends Cell Biol 14:20–28.

Sales, J., and G. P. J. Jassens. 2002. Nutrition of the domestic pigeon (*Columba livia domestica*). Worlds Poult. Sci. J. 59:221–232.

Schepers, L., P. Veldhoven, M. Casteels, H. J. Eyssen, and G. P. Mannaerts. 1990. Presence of three acyl-CoA oxidases in rat liver peroxisomes. An inducible fatty acyl-CoA oxidase, a noninducible fatty acyl-CoA oxidase, and a noninducible trihydroxyco-prostanoyl-CoA oxidase. J. Biol. Chem. 265:5242–5246.

Shetty, S., L. Bharathi, K. B. Shenoy, and S. N. Hegde. 1992. Biochemical properties of pigeon milk and its effect on growth. Comp. Biochem. Physiol. Part B: Biochem. Mol. Biol. 162:632–636.

Shetty, S., and S. N. Hegde. 1991. Changes in lipids of pigeon "milk" in the first week of its secretion. Lipids 26:930–933.

Shetty, S., P. V. Salimath, and S. N. Hegde. 1994. Carbohydrates of pigeon milk and their changes in the first week of secretion. Arch. Int. Physiol. Biochim. Biophys. 102:277–280.

Shetty, S., B. K. Shenoy, R. T. Jacob, and S. N. Hegde. 1990. Mineral composition of pigeon milk. Experientia 46:449–451.

Singh, B. K., M. Tripathi, B. P. Chaudhari, P. K. Pandey, and P. Kakkar. 2012. Natural terpenes prevent mitochondrial dysfunction, oxidative stress and release of apoptotic proteins during nimesulide-hepatotoxicity in rats. PLoS One 7:e34200.

Taylor, C. T. 2008. Mitochondria and cellular oxygen sensing in the HIF pathway. Biochem. J. 409:19–26.

Wan, X. P., P. Xie, Z. Bu, X. T. Zou, and D. Q. Gong. 2019. Prolactin induces lipid synthesis of organ-cultured pigeon crops. Poult. Sci. 98:1842–1853.

Wang, Y., X. Zhang, H. Yao, X. Chen, L. Shang, P. Li, X. Cui, and J. Zeng. 2022. Peroxisome-generated succinate induces lipid accumulation and oxidative stress in the kidneys of diabetic mice. J. Biol. Chem. 298:101660.

Wei, X. F., Q. G. Zhou, F. F. Hou, B. Y. Liu, and M. Liang. 2009. Advanced oxidation protein products induce mesangial cell perturbation through PKC-dependent activation of NADPH oxidase. Am. J. Physiol. Renal Physiol. 296:427–437.

Wen, J., X. Lin, S. Zheng, and Y. Xiao. 2020. Upregulation of Glutaredoxin 2 alleviates oxygen-glucose deprivation/reoxygenation-induced apoptosis and ROS production in neurons by enhancing Nrf2 signaling via modulation of GSK-3β. Brain Res 1745:146946.

Vandeputte-poma, J. 1980. Feeding, growth and metabolism of the pigeon, *Columba livia domestica*: duration and role of crop milk feeding. J. Comp. Physiol. 135:97–99.

Xie, P., M. X. Han, W. X. Chen, X. P. Wan, Y. G. Xu, and D. Q. Gong. 2020. The profiling of amino acids in crop milk and plasma and mRNA abundance of amino acid transporters and enzymes related to amino acid synthesis in the crop tissue of male and female pigeons during incubation and chick-rearing periods. Poult. Sci. 99:1628–1642.

Xie, P., X. P. Wan, Z. Bu, E. J. Diao, D. Q. Gong, and X. T. Zou. 2018. Changes in hormone profiles, growth factors and mRNA expression of the related receptors in crop tissue, relative organ weight, and serum biochemical parameters in the domestic pigeon (*Columba livia*) during incubation and chick-rearing periods under artificial farming conditions. Poult. Sci. 97:2189–2202.

Xie, P., X. P. Wang, Z. Bu, and X. T. Zou. 2017. Differential expression of fatty acid transporters and fatty acid synthesis-related genes in crop tissues of male and female pigeons (*Columba livia domestica*) during incubation and chick rearing. Br. Poult. Sci. 58:594–602.

Xie, P., J. G. Zhu, Y. Liu, T. W. Liu, Y. G. Xu, and D. Q. Gong. 2021. Effect of Akt activation on apoptosis-related gene expression in the crop tissues of male and female pigeons (*Columba livia*). Poult. Sci. 100:101392.

Yoon-Hee, H. 2015. ROS accumulation by PEITC selectively kills ovarian cancer cells via UPR-mediated apoptosis. Front. Oncol. 5:167.

Zhang, X., Y. Cui, L. Fang, and F. Li. 2008. Chronic high-fat diets induce oxide injuries and fibrogenesis of pancreatic cells in rats. Pancreas 37:e31–e38.

Zorov, D. B., M. Juhaszova, and S. J. Sollott. 2006. Mitochondrial ROS-induced ROS release: an update and review. Biochim. Biophys. Acta Bioenerg. 1757:509–517.